

## Down-regulation of osteopontin attenuates breast tumour progression *in vivo*

Goutam Chakraborty<sup>a</sup>, Shalini Jain<sup>a</sup>, Tushar V. Patil<sup>b</sup>, Gopal C. Kundu<sup>a, \*</sup>

<sup>a</sup> National Center for Cell Science, Pune, India

<sup>b</sup> Department of Histopathology, YCM Hospital, Pune, India

Received: November 13, 2007; Accepted: January 18, 2008

### Abstract

Development of breast tumour malignancies results in enhanced expression of various oncogenic molecules. Elevated expression of osteopontin (OPN) in higher grades of breast carcinoma correlates with enhanced expressions of several oncogenic molecules (urokinase-type plasminogen activator [uPA], matrix metalloproteinase-2/-9 [MMP-2 and -9]) and increased angiogenic potential of breast carcinoma. In this study, using *in vitro* and multiple *in vivo* models, we have demonstrated that silencing of OPN by its specific small interfering RNA (siRNA) down-regulates the expressions of oncogenic molecules such as uPA, MMP-2 and -9 resulting in inhibition of *in vitro* cell motility and *in vivo* tumorigenicity in mice. Moreover our results demonstrated that OPN<sup>-/-</sup> mice showed slower progression of tumour growth in breast cancer model as compared to wild-type mice. Furthermore, the data showed that injection of carcinogenic compound, pristane (2, 6, 10, 14-tetramethylpentadecane) induces breast tumour progression leading to enhanced expression of OPN and other oncogenic molecules in mammary fat pad of nude- and wild-type mice but not in OPN<sup>-/-</sup> mice. However, intratumoural injection of OPN siRNA to pristane-induced tumour significantly suppressed these effects. Our data revealed that knocking down of OPN effectively curb breast cancer progression and further suggested that developing of OPN-based therapeutics might be an emerging approach for the next generation of breast cancer management.

**Keywords:** osteopontin • pristane • breast tumour progression • angiogenesis

### Introduction

Metastatic spread of malignant cells to adjacent and distant sites makes cancer as the most dreaded disease. Recent evidences have indicated that diagnostic and prognostic markers play crucial roles during malignant progression and metastasis [1]. Osteopontin (OPN), a member of chemokines like, small integrin binding ligand N-linked glycoprotein (SIBLING) family of proteins [2, 3], plays an important role in determining the oncogenic potential of various cancers and is recognized as a key prognostic marker during the progression of cancer. OPN is an arginine-glycine-aspartate (RGD) containing adhesive glycoprotein [2] that expresses in a variety of tissues, including bone, dentin, cementum, kidney, vascular tissues, lymphocytes and in the specialized epithelia found in mammary glands [4, 5]. The role of OPN in the

regulation of tumour growth and angiogenesis is under intense investigation [6, 7].

Previously, Cook *et al.* have demonstrated that OPN induces multiple changes in gene expression that correlates with tumour progression in breast carcinogenesis model [8]. It has also been reported that highly metastatic human breast cancer cell lines express significantly higher levels of OPN as compared to the low metastatic ones [9]. Enhanced expression of OPN has been observed in the tissues as well as in the blood of the breast cancer patients [10]. Earlier observation demonstrated that suppression of OPN in MDA-MB-231 cells by its specific antisense S-oligonucleotide results in reduction of *in vitro* colony formation and *in vivo* osteolytic metastasis in nude rats [11]. Highly invasive cancers are characterized by aberrant activity of intra- or extracellular molecules such as protein kinases (tyrosine and serine), transcription factors and proteolytic enzymes [12]. The elevated nuclear factor kappa B (NF- $\kappa$ B)-DNA-binding has been detected in mammary carcinoma cell lines as well as in primary human breast cancer tissues, indicating the crucial role of NF- $\kappa$ B in breast cancer progression [13]. Earlier reports indicated that OPN

\*Correspondence to: Gopal C. KUNDU,  
National Center for Cell Science, Pune 411007, India.  
Tel.: 91-20-25708103  
Fax: 91-20-25692259  
E-mail: kundu@nccs.res.in

plays crucial role in activation of various kinases followed by NF- $\kappa$ B and activator protein (AP)-1 activation that ultimately triggers downstream effector gene expression, which controls breast cancer progression [2, 3]. In this study, we report that enhanced level of OPN expression in higher grades of breast tumours correlates with increased NF- $\kappa$ B activation, enhanced serine and tyrosine phosphorylation, which further correlated with elevated activation of matrix metalloproteinase-2/-9 (MMP-2/-9) and expression of urokinase-type plasminogen activator (uPA).

Several studies have indicated that small interfering RNA (siRNA) targeting to vascular endothelial growth factor (VEGF), epidermal growth factor receptor (EGFR) and other oncogenic molecules results in significant suppression of tumour progression [14–18]. Filleur *et al.* have reported that intratumoural injection of VEGF siRNA significantly slowed tumour vascularization and growth, which further indicated the potential use of *in vivo* siRNA-based approach in cancer therapeutics [14]. Accordingly, we hypothesized that intratumoural injection of siRNA specific to OPN could attenuate breast tumour growth in nude mice model.

Recent reports indicated that OPN produced either from tumour or stroma has been shown to enhance the metastatic potential of transformed cells [19]. The decreased rate of tumour invasion to bone was shown in OPN knockout mice as compared to wild-type mice [20]. Moreover recent finding indicated that OPN-knockout mice exhibit a significant delay of tumour development [21]. Therefore we sought to determine whether there is reduced breast tumour growth and neovascularization in OPN<sup>-/-</sup> mice compared to wild-type mice.

Pristane (2, 6, 10, 14-tetramethylpentadecane), a naturally occurring isoprenoid is considered as a potent carcinogen [22]. Previous reports have shown that intraperitoneal injection of pristane induces plasmocytomas in BALB/c mice [23–25]. It has also been reported that pristane can induce skin carcinogenesis [26]. Human breast adenocarcinoma (MCF-7) cells injected to the pristane primed mammary fat pad of virgin female Wistar rat causes development of solid tumours, which have been characterized as adenocarcinoma or fibroadenoma [27]. Pristane-induced tumours exhibit activation of several kinases such as protein kinase C (PKC) [25] and protein kinase A (PKA), enhanced activation of cAMP response element (CRE) [22] and c-Myc and increased expression of various molecules such as cyclooxygenase 2 (COX-2), prostaglandin E receptor (EP)-2, EP-4 and inducible nitric oxide synthases (iNOS) [28, 29]. In this study, we sought to determine the role of OPN in pristane-induced mammary tumourigenesis.

Here, using multiple *in vitro* and *in vivo* approaches, we have showed that OPN plays significant role in mammary carcinogenesis and our experimental data significantly correlated with the analysis of human breast clinical studies. Moreover, our study revealed that *in vivo* injection of OPN siRNA drastically reduced tumour growth. Furthermore, we have shown that the mice lacking OPN exhibit significant reduction of tumour growth. These data demonstrated, at least in part, that OPN could be a potential prognostic marker for the breast cancer progression and acts as key regulator of several other oncogenic molecules and further

suggested that targeting OPN might be a novel approach for the next generation of treatment of breast cancer.

## Materials and methods

### Materials

The rabbit anti-OPN polyclonal antibody was purchased from R & D Systems (Minneapolis, MN, USA). The anti-OPN antibody was also raised against purified intact human OPN in rabbit and characterized in our laboratory as described earlier [30]. Mouse anti-phosphotyrosine, rabbit anti-vWF (von Willebrand factor) antibodies and pristane were purchased from Sigma (St. Louis, MO, USA). Mouse anti-phosphoserine detection kit and anti-MT1-MMP antibody were obtained from Calbiochem (Darmstadt, Germany). Rabbit anti-p65 (NF- $\kappa$ B), anti-uPA, anti-MMP-9 antibodies and mouse anti-MMP-2, anti-p-Akt (Ser-473), anti-p-ERK (Tyr-204) antibodies, goat anti-actin antibody and siRNA transfection reagent were purchased from Santa Cruz Biotechnology (Santa Cruz, CA, USA). CA 15-3 antibody was obtained from Zymed (South San Francisco, CA, USA). The female athymic nude mice (NMR1, nu/nu) of 6–8 weeks of age were obtained from National Institute of Virology (Pune, India) and used in this study. Wild-type and OPN<sup>-/-</sup> (C57BL/6Jx129/SvJ, Strain name: B6.Cg-Spp1tm1Blh/J) mice were obtained from Jackson laboratory (Bar Harbor, ME, USA) and maintained at the National Center for Cell Science (NCCS; Pune, India) Experimental Animal Facility.

### Cell culture

Human breast adenocarcinoma cell line (MDA-MB-231) and non-virally transformed mice breast adenocarcinoma cell line, C1271 [31, 32], were obtained from American Type Culture Collection (Manassas, VA, USA). Cells were cultured in L-15 and Dulbecco's Modified Eagle Medium (DMEM) media, respectively, supplemented with 10% Fetal Bovine Serum (FBS), 100 (g/ml streptomycin and 100 units/ml penicillin).

### Human breast cancer specimen analysis

Human female breast tumour specimens and normal breast tissues were obtained from a local hospital with informed consent. Tissues were fixed in formaldehyde and paraffin blocks were prepared using standard protocols. Paraffin sections were used for histopathology and immunohistochemistry studies. Tumour grading was carried out by a modified Scarff–Bloom–Richardson (SBR) system with the help of an expert oncopathologist. Ten breast carcinoma specimens from each grade were used for analysis. Fresh tissues of various grades were also collected and used for electrophoretic mobility shift assay (EMSA).

### OPN-specific siRNA duplex

The siRNA duplexes targeting human OPN and scrambled siRNA are described in Table 1. The siRNA duplexes were synthesized by Dharmacon, Inc. (Lafayette, CO, USA). Each freeze-dried siRNA was reconstituted in RNase free water to prepare 20  $\mu$ M stock solution. The siRNAs were used for wound migration and *in vivo* tumourigenicity assays.

**Table 1** Osteopontin siRNA

OPNi 1	5' AUU UCA CAG CCA UGA AGA UdTdT/dTdT UAA AGU GUC GGU ACU UCU A 5'
Coni 1	5' CAG UAC AAC GCA UCU GGC AdTdT/ dTdT GUC AUG UUG CGU AGA CCG U 5'
OPNi 2	5'-CCA GUU GUC CCC ACA GUA GdTdT/ dTdT GGU CAA CAG GGG UGU CAU C-5'
Coni 2	5'-UCU UUC GAG CAA UCA GUU CdTdT/ dTdT AGA AAG CUC GUU AGU CAA G-5'
OPNi 3	5'-GCA GAC CCU UCC AAG UAA GdTdT/ dTdT CGU CUG GGA AGG UUC AUU C-5'
Coni 3	5'-GGA AUG UUC GGC UGC CUA UdTdT/ dTdT CCU UAC AAG CCG ACG GAU A-5'
OPNi 1 Single mismatch (SM)	5'AUU UCA CAG CCA UGA AGA UdTdT/ dTdT UAA AGU GUC GGU ACU UCU A 5'
OPNi 1 Double Mismatch (DM)	5'AUU UCA CAG CCA UGA AGA UdTdT/ dTdT UAA AGU GUC GCA ACU UCU A 5'

### Western blot analysis and EMSA

Western blot and EMSA were performed as described [33, 34].

### Wound migration assay

Wound assay was performed using transfected or non-transfected MDA-MB-231 cells as described [7].

### Gelatin zymography

To determine the gelatinolytic activity of MMP-2 and MMP-9, gelatin zymography was performed using tumour tissue lysates as described earlier [35].

### *In vivo* xenograft model

MDA-MB-231 ( $5 \times 10^6$ ) cells were injected orthotopically into the left inguinal mammary fat pad of female nude mice (NMR1) ( $n = 6/\text{group}$ ). After 1 week, OPN-specific siRNA (250  $\mu\text{g}/\text{kg}$  body weight/mouse) was mixed with siRNA transfection reagent and injected intratumourally as described [14, 36], thrice in a week until the completion of experiments. Control group of mice was injected with transfection reagent along with control OPNi 1 (Coni). Animals were kept in pathogen free conditions and monitored regularly. After 8 weeks, mice were sacrificed by cervical dislocation and photographed. Primary breast tumours were dissected out and weighed. One part of the tumours were fixed in 10% formalin solution and used for histopathology and immunohistochemistry. The other part was snap frozen and used for EMSA.

### Generation of breast tumour in wild-type and OPN knockout mice

Mouse breast adenocarcinoma C1271 ( $5 \times 10^6$ ) cells were mixed with 500- $\mu\text{l}$  cold growth factor depleted Matrigel and injected orthotopically to the left inguinal mammary fat pad of female wild-type (OPN<sup>+/+</sup>) and knockout (OPN<sup>-/-</sup>) mice ( $n = 6/\text{group}$ ). The mice were kept in the pathogen-free condition for 8 weeks. After termination of experiments, mice were sacrificed; photographed, primary breast tumours were dissected out, weighed and analysed as described earlier.

### Generation of pristane-induced mammary tumourigenesis in mice

Pristane was injected in the left inguinal mammary fat pad of female nude mice, thrice in a week for up to 6 weeks. After that, mouse OPN siRNA (mOPNi) (250  $\mu\text{g}/\text{kg}$  of body weight/mouse) mixed with transfection reagent was injected directly into the pristane-induced tumour thrice in a week for subsequent 6 weeks as described above. After 12 weeks, mice were sacrificed and mammary fat pad was dissected out and used for histopathology and immunohistochemical analysis.

In separate experiments, pristane was injected (thrice in a week) to the left inguinal mammary fat pad of female wild-type (OPN<sup>+/+</sup>) and knockout (OPN<sup>-/-</sup>) mice ( $n = 6/\text{group}$ ). Mice were kept until development of tumour (16 weeks) and then sacrificed, photographed and tumours in mammary fat pad were dissected out for further analysis.

### Immunofluorescence analysis

Immunofluorescence studies of human and mice tumours were performed as described earlier [34, 37].

### Statistical analysis

The bands were analysed densitometrically (Kodak Digital Science, USA) and fold changes were calculated. The expressions of OPN, uPA, MMP-2, MMP-9 and vWF in human clinical specimens were quantified using the Image Pro Plus 6.0 software (Nikon, Japan) and expressed as mean  $\pm$  SE. The mouse tumour weights were measured and plotted in the form of a bar graph. Statistical differences were determined by Student's *t*-test. Differences were considered significant when the *P*-value was less than 0.05.

## Results

### Expression profiles of OPN, NF- $\kappa$ B, uPA, MMP-2 and -9, MT1-MMP and vWF in different grades of human breast cancer specimens and its correlation with tumour progression and angiogenesis

The various histologic grades of breast carcinomas provide clinically important prognostic information [38]. The expression

profile of different genes is related to the molecular basis of histological grades and it helps to improve the prognosis of breast cancer [38]. Because OPN is considered as a metastasis-associated gene and plays a crucial role in determining the oncogenic potential of several cancers including breast [2, 3], we sought to determine the expression profiles of OPN and other oncogenic molecules in different grades of human breast carcinoma. Breast tumour clinical specimens were collected from a local hospital with informed consent and their gradations were analysed by a modified SBR system ( $n = 10/\text{group}$ ). Figure 1A, panel I, represents the typical haematoxylin and eosin stained histopathological photographs of breast carcinoma of different grades. The level of OPN in different grades has been determined by immunofluorescence and analysed by Image Pro Plus 6.0 software (Nikon) and represented graphically (Fig. 1A, panel II and Fig. 1B). The data showed that the expression profile of OPN was significantly higher in grades II and III as compared to grade I and normal samples (Fig. 1A, panel II) and it is localized in both lobular and epithelial parts in higher grades of tumours. Thus the expression profile of OPN was correlated with the different clinicopathological features of breast cancer specimens with SBR gradation (*i.e.* percentage of lobules, number of mitotic features/hpf and nuclear polymorphism). Moreover, the status of total serine and tyrosine phosphorylations was considerably higher in grade II and III tumours, which further correlates with OPN overexpression in these clinical specimens (Fig. 1A, panels III and IV).

We have examined the cellular localization of NF- $\kappa$ B in different grades of breast tumour tissues. In normal breast tissue or lower grades, distinct cytoplasmic localization of p65 subunit of NF- $\kappa$ B was observed (Fig. 1A, panel V, as indicated by red arrows) whereas in grade III specimens, significant nuclear localization of p65 was found (as shown by white arrows). In grade II specimens, both cytoplasmic and nuclear localization of p65 was observed. The NF- $\kappa$ B-DNA binding was determined by EMSA, which correlates with immunofluorescence study (Figs. 1A and C). These data suggested the correlation between enhanced OPN expression and NF- $\kappa$ B activation, which is associated with enhanced malignancies in breast carcinoma. It has been reported that OPN induces AP-1 activation in breast cancer cells [2]. In this study, we observed the elevated AP-1-DNA-binding in higher grades of specimens (Fig. 1D). The expression profiles of uPA, MT1-MMP, MMP-2 and MMP-9 were analysed by immunohistochemistry by using their specific antibodies (Fig. 1A, panels VI–IX) and represented in the form of a bar graph (Fig. 1B). The elevated expressions of these molecules were observed in higher grades of tumours compared to normal tissue or lower grade of tumours. Interestingly, we have observed that the expression profiles of uPA and MMP-9 were considerably higher in grades II and III, whereas the enhanced levels of MMP-2 and MT1-MMP were detected in grade III tumours. The enhanced expression of vWF in grades II and III tumours suggested the increased angiogenic potential in higher grades of tumours (Fig. 1A, panel X and Fig. 1B). The expression profile of OPN, uPA, MMP-9, MMP-2 and vWF were normalized with respect to 4',6-diamidino-2-phenylindole (DAPI) in these tumours. Taken together, our data demonstrated that enhanced expression of OPN

correlates with higher expression/activation profiles of uPA, MT1-MMP, MMP-2 and MMP-9, NF- $\kappa$ B and AP-1 and enhanced neovascularization, suggesting that OPN might be considered as an important prognostic marker for breast cancer progression.

### **Silencing of tumour-derived OPN suppresses the activation and expression of NF- $\kappa$ B, AP-1, ERK, Akt, MMP-2, MMP-9 and uPA and inhibits breast cancer cell motility *in vitro***

To examine the role of tumour-derived OPN in regulation of downstream signalling molecules and cell motility, MDA-MB-231 cells were transfected with three different OPN siRNAs (OPNi) designed from three specific regions as described in Table 1. The OPN expression was determined by Western blot and the data indicated that OPNi 1 but not OPNi 2 and OPNi 3 specifically suppressed OPN expression (Fig. 2A). To further examine the specificity of OPNi 1, single and double mismatched OPN siRNAs containing either one or two central mismatch was synthesized (Table 1). Our data revealed that single and double mutants were unable to suppress OPN expression, which further showed the specificity of OPNi 1 (Fig. 2B). Accordingly, OPNi 1 was referred as OPNi and used throughout the study. To examine the role of tumour-derived OPN in regulation of downstream signalling molecules, MDA-MB-231 cells were transfected with OPNi and the levels of pERK, pAkt, uPA, MMP-2 and -9 and NF- $\kappa$ B and AP-1-DNA binding were detected by Western blot and EMSA, respectively. The results showed that silencing tumour-derived OPN down-regulates phosphorylations of ERK and Akt, and expressions of uPA, MMP-2 and -9 (Fig. 2C) and inhibited NF- $\kappa$ B- and AP-1-DNA binding (Fig. 2D, panels I and II) in these cells. To study the effect of tumour-derived OPN on breast tumour cell motility, MDA-MB-231 cells were transfected with OPNi or Coni and wound migration assay was performed. Wound photographs were taken at 0 and 12 hrs and the results indicated that silencing OPN significantly reduced breast tumour cell wound motility (Fig. 2E).

### **Silencing tumour-derived OPN abrogates breast tumour growth and MMP-2, MMP-9 and uPA expression in nude mice model**

To investigate the role of tumour-derived OPN in the *in vivo* xenograft tumour growth, MDA-MB-231 cells were implanted in the mammary fat pad of female nude mice. OPNi and Coni (*i.e.* Coni1) were injected intratumourally as described in 'Materials and methods'. After 8 weeks, mice were sacrificed and the tumours were dissected out, photographed, weighed and analysed statistically and represented in the form of a bar graph ( $*P < 0.02$ ) (Fig. 3A). The data indicated that OPNi significantly reduced the breast tumour load as well as growth characteristics in nude mice. Figure 3B, panels I and II, showed the typical histopathological morphology of mouse mammary tumours (10 $\times$  and 60 $\times$  magnification). The data indicated that xenograft tumours exhibit poorly

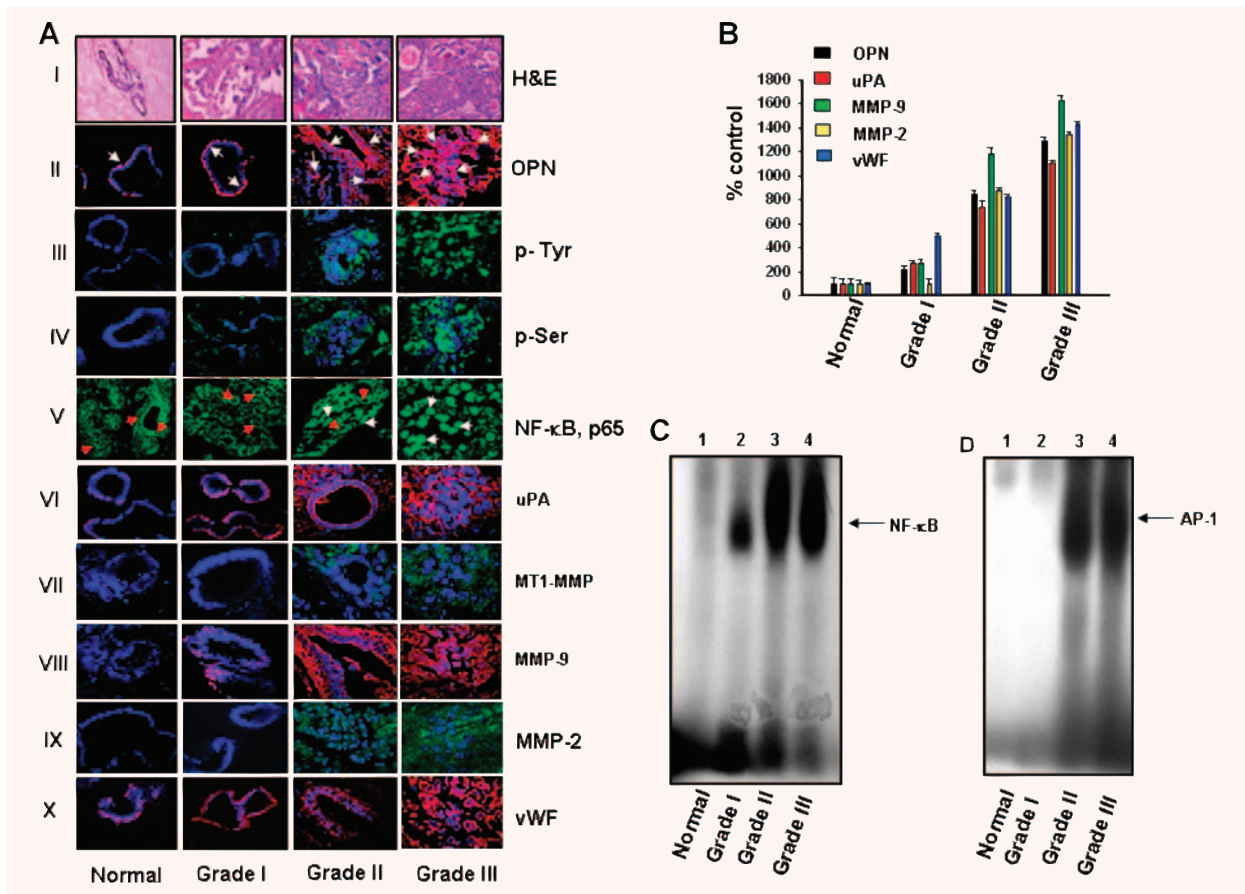


**Fig. 1** Expression profiles of OPN and other oncogenic molecules in the human breast tumour specimens of different grades. (A) typical photographs (haematoxylin and eosin stained) of human breast tumour specimens of different grades (panel I). Breast tumour specimens were stained with rabbit anti-OPN antibody followed by Cy-3-conjugated anti-rabbit IgG (red). Note that the expression of OPN is shown by arrows (panel II). Status of total tyrosine and serine phosphorylations were determined by immunohistochemistry by using anti-mouse phosphotyrosine or phosphoserine antibody followed by FITC-conjugated anti-mouse IgG (green) (panels III and IV). Nuclear localization of NF- $\kappa$ B, p65 were visualized in grade II and III specimens and indicated by white arrows whereas cytoplasmic localization of p65 was observed in normal and grade I specimens and indicated by red arrows (panel V). The levels of uPA (panel VI), MT1-MMP (panel VII), MMP-9 (panel VIII) and MMP-2 (panel IX) in different grades of breast tumour specimens were detected by immunohistochemical studies using their specific antibodies. The neovascularization was visualized by using anti-vWF antibody (panel X). NF- $\kappa$ B, p65, MT1-MMP and MMP-2 were stained with FITC-conjugated anti-mouse IgG (green), whereas uPA, MMP-9 and vWF were stained with Cy3-conjugated anti-rabbit IgG (red). Nuclei were stained with DAPI (blue). Note that the expression of all these molecules and neovascularization are significantly higher in grade II and grade III specimens. (B) The expression profiles of OPN, uPA, MMP-2, MMP-9 and vWF in various grades of breast tumour specimens were quantified using Image Pro Plus software (Nikon) and represented graphically ( $n = 10/\text{grade}$ ). The expression profile of these molecules were normalized with respect to DAPI. (C and D) The NF- $\kappa$ B and AP-1 DNA-binding in different grades were analysed by EMSA. Note that significantly enhanced DNA-binding was observed in higher grades of tumour specimens.

differentiated structure in mammary fat pad. However, well-differentiated lobular structures were observed in OPNi-injected mammary fat pad of xenograft tumours (shown by blue arrows) indicating that silencing tumour-derived OPN reduces tumourigenicity. The characteristics of mice xenograft tumours are summarized in Table 2. Immunohistochemical analysis indicated that the expression profiles of OPN, MMP-2, MMP-9, MT1-MMP and uPA were significantly reduced in OPNi-injected xenograft tumours (Fig. 3B, panels III and IV and Fig. 3C, panels I–III). Interestingly, the phosphory-

lation (serine and tyrosine) status of xenograft tumours of mice was drastically down-regulated in presence of OPN siRNA (Fig. 3C, panels IV and V). We have demonstrated earlier in this paper that increased serine and tyrosine phosphorylation correlates with enhanced tumourigenicity in human breast carcinoma specimens (Fig. 1A, panels III and IV). These data suggested that suppressing tumour-derived OPN not only down-regulates expressions of uPA and MMP-2/9 but also inhibits total phosphorylations of tyrosine and serine residues of signalling molecules, which ultimately curb

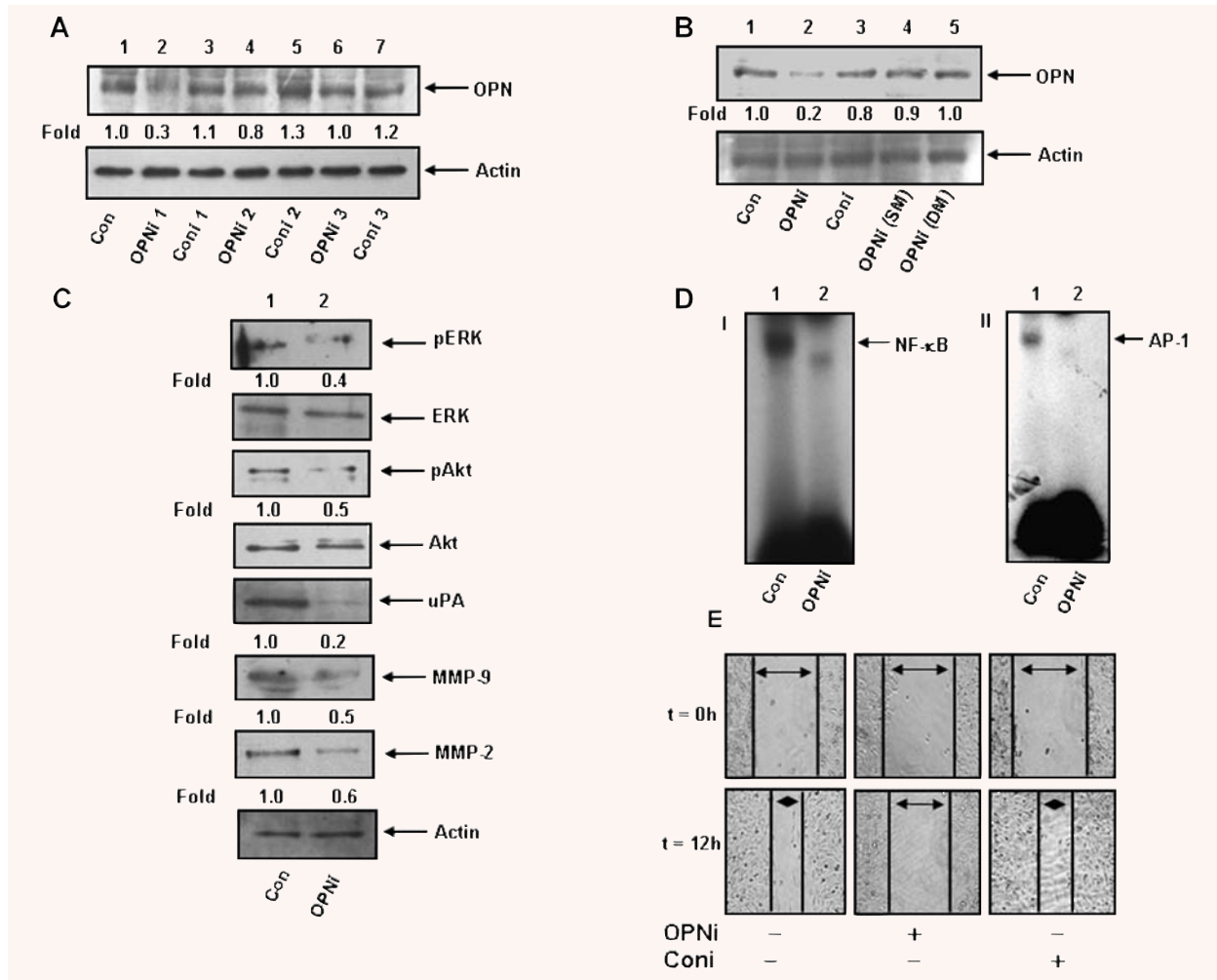


**Fig. 2** (A and B) MDA-MB-231 cells were transfected with various OPN-specific siRNA (OPNi, see Table 1) and OPN expression was detected by Western blot. Actin was used as loading control. (C) Cells were transfected with OPNi (OPNi1). The levels of pERK, pAkt, uPA, MMP-9 and MMP-2 in cell lysates were analysed using their specific antibodies. Non-phospho ERK, Akt and actin were used as loading controls. Fold changes were calculated. (D) DNA binding of NF- $\kappa$ B (panel I) and AP-1 (panel II) were performed from the nuclear extract obtained from control or OPNi transfected MDA-MB-231 cells. (E) Cells were transfected with OPNi or Coni. Wounds of constant diameter were made and wound assay was performed. Photographs were taken at 0 and at 12 hrs under Nikon microscope. The data represent three experiments exhibiting similar results.

breast tumour progression. Moreover, our data also showed that there was reduction of nuclear localization of NF- $\kappa$ B in the OPNi-injected tumours (Fig. 3C, panel VI). EMSA data support these findings and showed that OPNi reduced NF- $\kappa$ B and AP-1-DNA binding (Fig. 3D, panels I and II). Recent studies have revealed that OPN plays crucial role in tumour angiogenesis [3]. Therefore to determine whether silencing of OPN results in suppression of angiogenesis in breast tumour model, the mice xenograft tissue sections were stained with anti-vWF (an endothelial cell specific marker) antibody and visualized under confocal microscopy. The results indicated that vWF expression in xenograft tumour was drastically reduced in presence of OPNi (Fig. 3C, panel VII). These results clearly demonstrated that tumour-derived OPN plays crucial

role in regulation of tumour progression and angiogenesis because targeting OPN by its specific siRNA suppresses the expression of oncogenic molecules and down-regulates the neo-vascularization that ultimately abrogates tumour progression.

### Deficiency of host OPN reduces breast tumour growth and suppresses the expression of oncogenic molecules in OPN knock out mice model

To assess breast tumour development in OPN-deficient mice, mice breast adenocarcinoma C1271 cells were mixed with growth factor depleted Matrigel as described earlier and implanted orthotopically

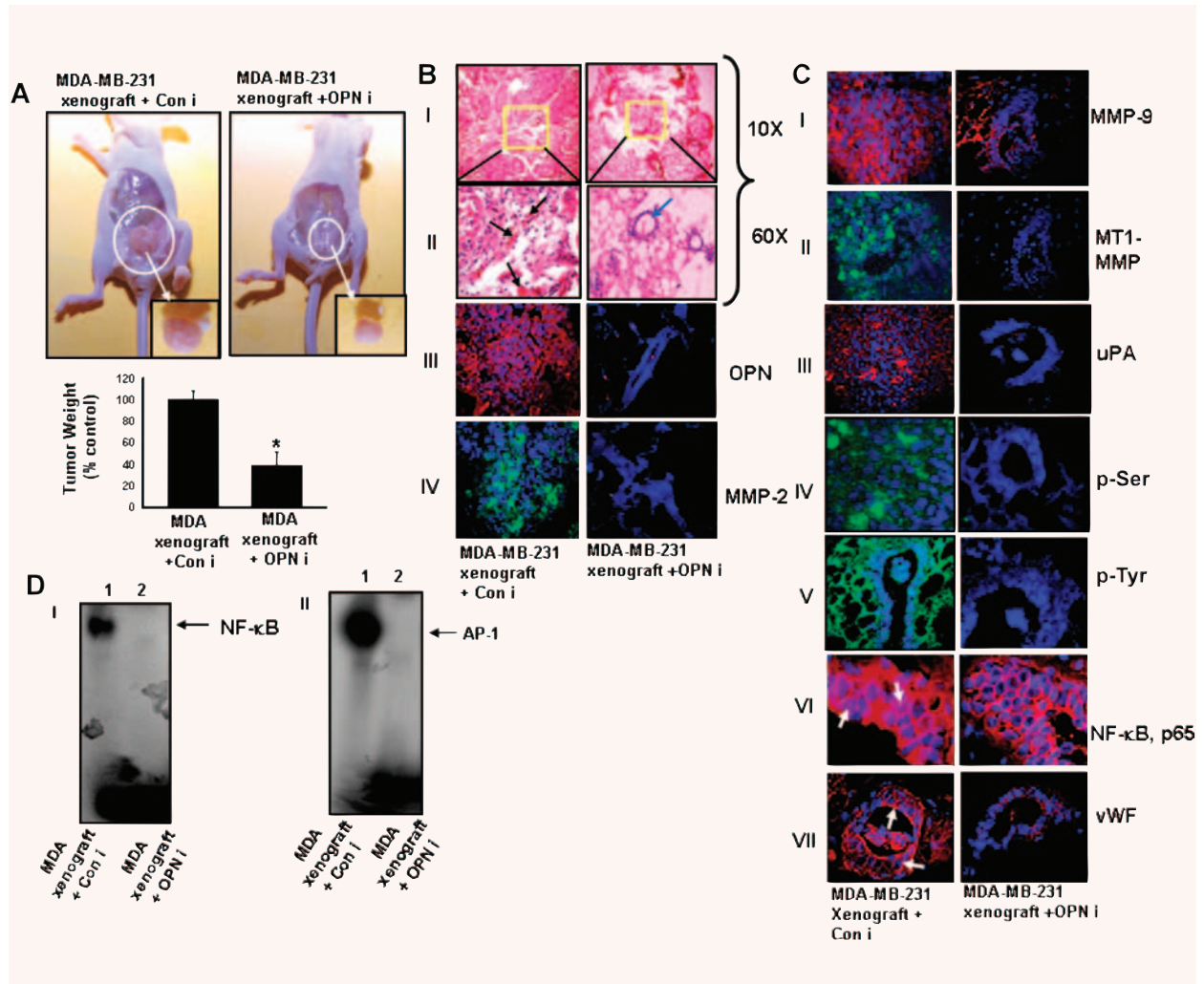


**Fig. 3** OPN-specific siRNA suppresses breast tumour progression and angiogenesis in nude mice. **(A)** MDA-MB-231 ( $5 \times 10^6$ ) cells were injected orthotopically into the left inguinal mammary fat pad of female nude mice (NMRI) ( $n = 6$ /group). After 1 week, OPN-specific siRNA ( $250 \mu\text{g/kg}$  body weight/mouse) was mixed with siRNA transfection reagent and injected intratumorally, thrice in a week until the completion of experiments. Control group of mice was injected with transfection reagent along with control OPN siRNA 1 (Coni). Typical photographs of orthotropic xenograft tumours are shown (upper panel). Isolated tumours are shown in inset. Note that intratumoural injection of OPNi but not Coni significantly reduced tumour load. Lower panel: The tumour weights were quantified and represented in the form of a bar graph ( $*P < 0.02$ ) ( $n = 6$ ). **(B and C)** Histopathology (haematoxylin and eosin) of the mice breast tumour section. Photographs were taken in  $10\times$  and  $60\times$  magnification **(B, panels I and II)**. Blood vessels in the tumour section were indicated by black arrows whereas the typical breast lobular structure in OPNi-injected tumours were indicated by blue arrow. Expression profiles of OPN, MMP-2, MMP-9, MT1-MMP and uPA were detected by immunohistochemical studies **(B, panels III and IV and C, panels I–III)**. OPN, MMP-9 and uPA were stained with Cy-3 whereas MT1-MMP was stained with FITC. Nuclei were stained with DAPI. Status of total phosphorylations were shown using anti-phosphoserine and anti-phosphotyrosine antibodies followed by staining with FITC-conjugated IgG **(C, panels IV and V)**. Cellular localization of NF- $\kappa$ B, p65 and expression of vWF (neovascularization) were shown by immunofluorescence using their specific antibodies followed by staining with Cy3 conjugated IgG (panels VI and VII). **(D)** EMSA analysis of NF- $\kappa$ B (panel I) and AP-1 (panel II)-DNA binding in tumour tissues.

to the left inguinal mammary fat pad of wild-type and OPN<sup>-/-</sup> mice. Mice were kept for 8 weeks and then sacrificed. The data indicated that there were significant reductions of breast tumour growth in OPN<sup>-/-</sup> mice (>5.5 fold) as compared to wild-type mice

(Fig. 4A). These data suggested that host OPN also played important role in regulation of breast tumour growth. Histopathological analysis of tumour tissue sections showed that there were significantly higher cellular infiltration, nuclear polymorphism and poorly

**Table 2** Characteristics of MDA-MB-231 orthotropic xenograft tumor in nude mice

Tumor characteristics	MDA-MB-231 xenograft	MDA-MB-231 xenograft + OPN siRNA
Tumor infiltration	Significant enhanced levels of infiltration	Poor infiltration
Tumor differentiation	Poorly differentiated structure, 20–40% mammary fat pad lobules	Well differentiated lobular structure
Vessel formation	High, more vWF positive	Poor, less vWF positive
Mitotic features/ hpf	7–9	1–3
Tumor giant cell	Plenty	Scanty
Nuclear polymorphism	Significant nuclear size variation	Small regular and uniform nucleus

differentiated structure in tumour of wild-type mice as compared to OPN<sup>-/-</sup> mice (Fig. 4B, panels I and II). The expressions of MMP-9, MMP-2, uPA and MT1-MMP were also detected by immunohistochemistry and the data showed that the expression levels of all these molecules are significantly down-regulated in OPN<sup>-/-</sup> mice (Fig. 4B, panels IV–VII). Moreover, reduction in tumour vascularization was observed in OPN<sup>-/-</sup> mice (Fig. 4B, panel VIII). The level of OPN expression in tumour lysates was detected by Western blot and the gelatinolytic activity of MMP-2 and MMP-9 were examined by zymography. The data showed that there were significant reductions of OPN expression (Fig. 4C) and MMP-2 and MMP-9 activation (data not shown) in tumour developed in OPN<sup>-/-</sup> mice as compared to wild-type mice. Our data also showed the drastic reduction of NF- $\kappa$ B and AP-1-DNA binding in tumours of OPN<sup>-/-</sup> mice, which further indicated that loss of NF- $\kappa$ B and AP-1 activation was OPN dependent (Fig. 4D). These data indicated that lack of host OPN expression resulted in reduced expressions of various oncogenic molecules such as MMPs, uPA and down-regulated the activations of NF- $\kappa$ B and AP-1 that ultimately suppressed breast tumour growth and angiogenesis.

### Pristane induces OPN-dependent mammary tumourigenesis in nude mice

Exposure with external carcinogen is known to induce tumours. Recently it has been reported that carcinogenic compound such as asbestos induces expression of OPN in patients with pleural mesothelioma [39]. To examine the role of external carcinogen in mammary tumourigenesis, we injected pristane, a known natural carcinogen to the mammary fat pad of nude mice and observed that there was significant induction of tumour growth. To determine the role of OPN in pristane-induced breast tumourigenesis, mOPNi was injected intratumourally into the pristane-induced tumours and the data showed that OPNi inhibits pristane-induced mammary tumourigenesis. Tumour weights were measured and the data indicated that injection of mOPNi reduced more than 60% of tumour weight in mice (data not shown). The mammary tumours were also analysed by histopathology. The micrographs of the tumour sections were

taken under microscope (10 $\times$  and 60 $\times$  magnifications) (Fig. 5A, panels I and II). The characteristics of these tumours are described in Table 3. The injection of pristane into the mammary fat pad of nude mice showed poorly differentiated structure with high nuclear polymorphism and large number of mitotic features (Table 3). Enhanced vascularization was observed in pristane induced but not in OPNi-injected tumours (Fig. 5A, panels II, indicated by arrows). Immunohistochemical studies with anti-OPN antibody showed that there was marked induction of OPN expression in pristane-induced tumours (Fig. 5A, panel III). These data indicated that injection of pristane resulted in enhanced breast tumour load in nude mice whereas direct delivery of OPNi to the site of pristane-induced tumours showed reduction of the breast tumour growth (Table 3).

These findings prompted us to analyse the expression and activation status of various oncogenic molecules and transcriptions factors in these tumour samples. The results indicated the high levels of MMP-9, MMP-2, MT1-MMP and uPA expressions in pristane-induced tumours compared to normal mammary fat pad of nude mice (Fig. 5A, panels IV–VI and Fig. 5B, panel I). OPNi drastically suppressed the pristane-induced expression of these molecules in tumours. Furthermore, the data suggested that pristane not only induced the nuclear localization of NF- $\kappa$ B, p65 (indicated by arrows) but also enhanced its DNA binding (Fig. 5B, panel II and Fig. 5C, upper panel). OPNi suppressed the pristane-induced NF- $\kappa$ B nuclear translocation, NF- $\kappa$ B and AP-1-DNA binding (Fig. 5B, panel II and Fig. 5C, upper and lower panels). Moreover, the total phosphorylations of serine and tyrosine residues of signalling molecules were significantly higher in pristane-induced tumours compared to control or OPNi-injected tumours (Fig. 5B, panels III and IV). Previous reports have indicated that ERK and Akt (tyrosine- and serine-specific kinases) play crucial role in OPN-induced signalling in various cancers [2]. Therefore, we sought to determine the status of phosphorylations of these kinases in pristane-induced mammary tumours and our data revealed that there were marked inductions of phosphorylations of ERK and Akt in pristane-induced tumours but not in OPNi-injected tumours (Fig. 5B, panels V and VI). Elevated expression of vWF was also observed in pristane-induced mammary tumours (Fig. 5B, panel VII). However, OPNi inhibits vWF

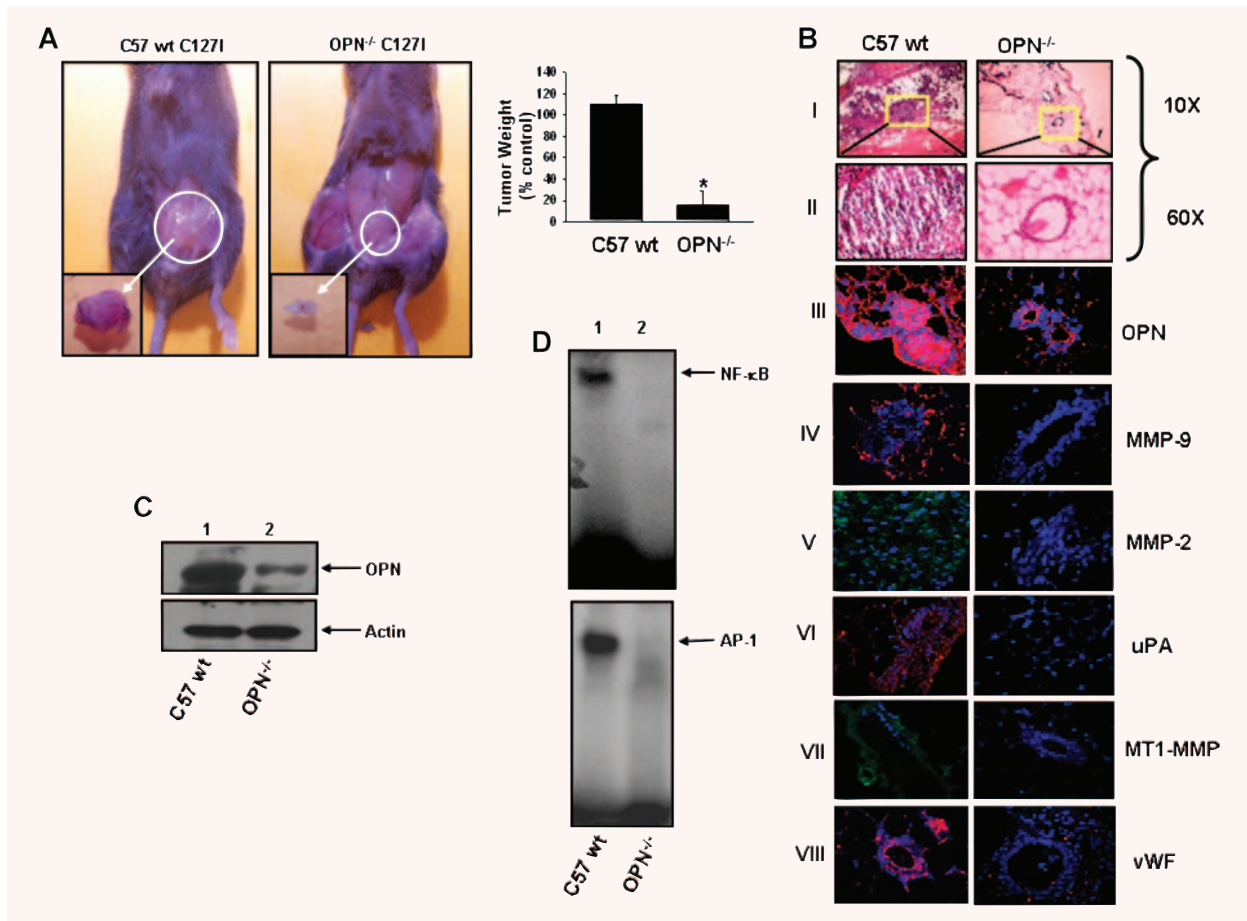


**Fig. 4** Deficiency of host OPN reduces orthotopic breast tumour growth in  $OPN^{-/-}$  mice. **(A)** Typical photographs of orthotopic breast tumours in wt and  $OPN^{-/-}$  mice. Isolated tumours are shown in inset. Tumour weights are represented graphically ( $n = 6$ ) ( $*P < 0.04$ ). **(B)** Histopathological (haematoxylin and eosin) analysis of mice tumours. Photographs were taken in 10 $\times$  and 60 $\times$  magnifications (panels I and II). The expressions of OPN (panel III), MMP-9 (panel IV), MMP-2 (panel V), uPA (panel VI), MT1-MMP (panel VII) and vWF (panel VIII) in mice tumours were detected by immunohistochemistry using their specific antibodies. OPN, MMP-9, uPA and vWF were stained with Cy-3 whereas MT1-MMP and MMP-2 were stained with FITC. Nuclei were stained with DAPI. A higher vWF expression was observed in wild-type but not in  $OPN^{-/-}$  mice tumours indicated the OPN deficiency suppresses tumour neovascularization. **(C)** The expression of OPN in tumour lysates was detected by Western blot. Actin was used as control. **(D)** NF- $\kappa$ B and AP-1-DNA binding in wild-type and  $OPN^{-/-}$  mice tumours were determined by EMSA.

expression in these tumours, which further indicated that pristane promotes OPN-dependent mammary tumourigenesis through the induction of angiogenesis.

### Reduced progression of pristane-induced tumour growth and angiogenesis in OPN-deficient ( $OPN^{-/-}$ ) mice

Our previous findings prompted us to determine the effect of pristane on breast tumourigenesis in wild type (wt) and  $OPN^{-/-}$

mice. Accordingly, pristane was injected in the mammary fat pad of wt and  $OPN^{-/-}$  mice. After termination of experiments, mice were sacrificed. Figure 6A shows the typical photographs of mice with breast tumours. Our data revealed that there was significant reduction of breast tumour growth (~65%) in  $OPN^{-/-}$  mice as compared to wt mice (Fig. 6A). The tumour sections were analysed histopathologically and the data indicated that there was significant loss of tumourigenicity (less infiltration, well-differentiated structure, reduced mitotic feature) in the  $OPN^{-/-}$  mice, whereas enhanced tumourigenesis was observed in pristane-induced wt mice (*i.e.* enhanced infiltration, poorly differentiated structure,

**Table 3** Characteristics of pristane-induced mammary fat pad tumor in nude mice

Tumor characteristics	Normal mammary fat pad	Pristane injected mammary fat pad	Pristane + mOPN siRNA
<b>Tumor infiltration</b>	No infiltration	Higher level of cellular infiltration	Less infiltration
<b>Tumor differentiation</b>	Well differentiated normal mammary fat pad structure	Very poorly differentiated structure. Lobular structure almost absent	Moderately differentiated with 60–80% lobules
<b>Vessel formation</b>	Less, rarely observed vWF positive areas	Enhanced vWF positive areas indicating more neovascularization	vWF positive areas depleted
<b>Mitotic features/ hpf</b>	–	10–12/hpf	4–5/hpf
<b>Tumor giant cell</b>	No tumor giant cells.	Plenty	Scanty
<b>Nuclear polymorphism</b>	Small regular and uniform nucleus	Marked nuclear size variation	Moderate nuclear size variation

more mitotic feature, enhanced vasculature) (Fig. 6B, panels I and II). The level of OPN expression was almost absent in tumours of OPN<sup>-/-</sup> mice (Fig. 6B, panel III). The pristane-induced tumours in wild-type but not OPN<sup>-/-</sup> mice were positive to CA-15-3 (breast tumour marker) (Fig. 6B, panel IV) suggesting that these are indeed breast tumours. The expressions of MMP-9, uPA and vWF were significantly higher in tumours of wt mice as compared to OPN<sup>-/-</sup> mice (Fig. 6B, panels V-VII). The gelatinolytic activity of MMP-2 and MMP-9 were detected by zymography from the tumour lysate (Fig. 6C). The data showed that there was significant reduction of MMP-2 and MMP-9 activation in pristane-induced tumours of OPN<sup>-/-</sup> mice as compared to wild-type mice (Fig. 6C). Enhanced NF- $\kappa$ B and AP-1-DNA bindings were also observed in wild-type but not in OPN<sup>-/-</sup> mice (Fig. 6D). Taken together, our data indicated that pristane-induced breast tumours were significantly suppressed in absence of host OPN, which indicated that OPN plays crucial roles in this process.

## Discussion

Tumour progression is a series of complex events that requires the interplay among various cytokines, kinases, transcription factors, proteases and oncogenic molecules. Recent studies have indicated that OPN acts as a key regulator of tumour progression through activating several signalling cascades, growth factors and inducing the expression of several oncogenic molecules [2, 3]. Thus we hypothesized that targeting OPN might be a novel approach to suppress the metastatic potential of cancers. In this study, we showed that silencing of OPN expression significantly down-regulates breast tumour progression in xenograft models. Moreover, we observed the higher expression of OPN in pristane-induced tumours and silencing of OPN expression by OPNi

significantly abrogates pristane-induced mammary tumorigenesis in nude mice models. Interestingly, the breast tumour model in OPN<sup>-/-</sup> mice showed slower progression of tumour growth as compared to wt mice. Using four independent mice models, we have demonstrated that OPN either produced in tumour and/or stromal environment plays a crucial role in regulation of breast tumour growth and angiogenesis.

Although various therapeutic approaches have been recently implicated for the anti-cancer therapy, there are several accidental side effects of these approaches (*i.e.* chemotherapy, radiotherapy, etc.) that may cause severe physiological disorder which might reduce the chances of survival of the patients. Therefore, the recent concept of cancer therapy is directed towards targeting the molecule that is involved in regulation of metastatic signature or angiogenic switch [40–42]. Recent studies have suggested that expression profiling of various gene may provide the molecular basis of histological grade to improve prognosis and treatment of breast cancers [38]. Earlier reports have indicated that OPN acts as most potent metastasis-associated gene and plays important roles in regulation of tumour angiogenesis and considered as the potent oncogenic marker during breast cancer progression [3]. Thus targeting OPN at transcriptional or protein level or blocking its receptor or its downstream signalling pathways could be an emerging approach for anti-cancer therapy [43, 44]. In recent times, intratumoural delivery of siRNA showed great prospect in cancer therapy particularly in *in vivo* mice model [14, 36]. In this study, we design a small interfering RNA (siRNA) against OPN and demonstrate that intratumoural injection of siRNA significantly suppressed breast tumour growth and angiogenesis in the mouse model.

Exposure of the external carcinogen is one of the major causes of cancer development. It is well established that exposure of external carcinogens results in alteration of several gene expression and activation of oncogenes that ultimately induce cancer progression [45]. These reports prompted us to determine the effect of OPN-specific siRNA in carcinogen-induced tumorigenesis

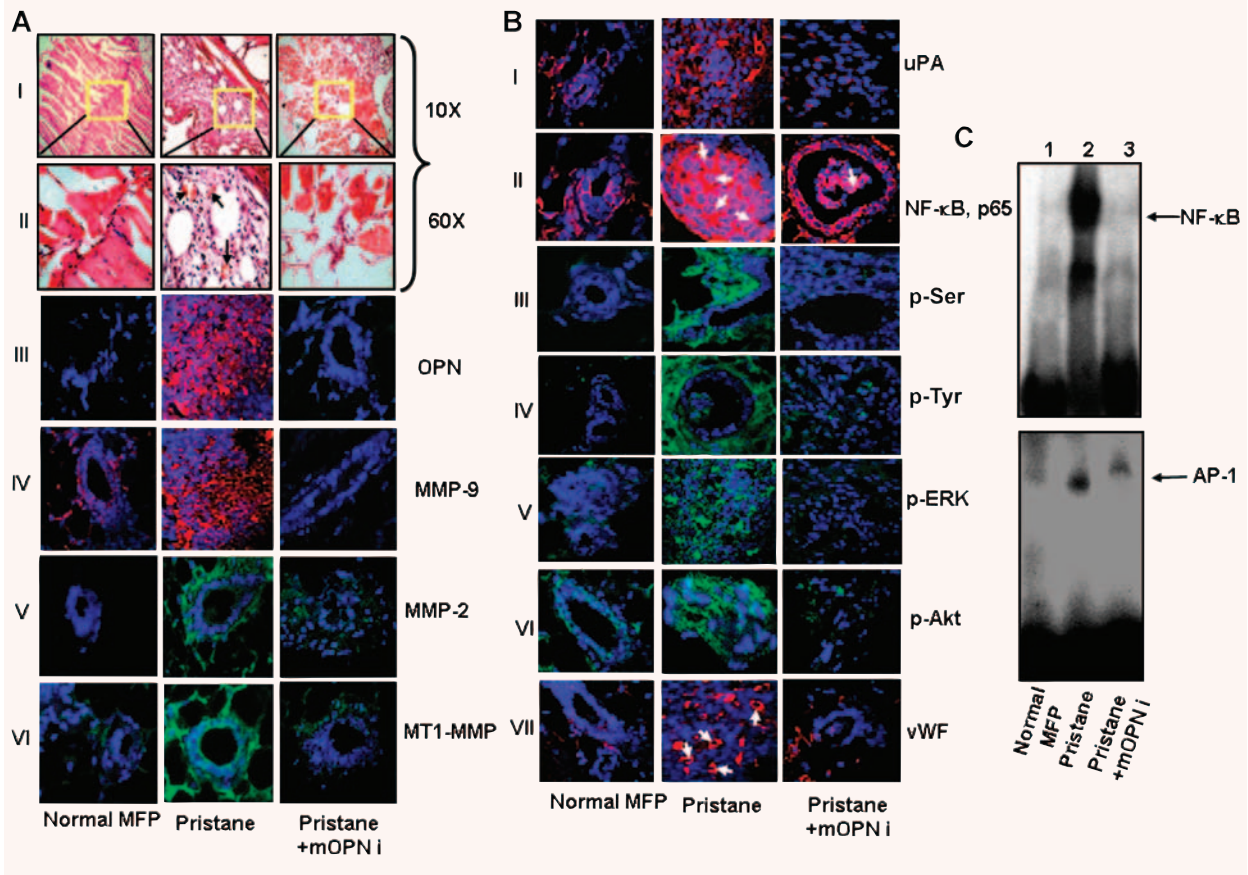


**Fig. 5** Silencing of OPN significantly down-regulates pristane-induced mammary carcinogenesis in nude mice. **(A)** Haematoxylin and eosin staining showed the mammary carcinogenesis induced by pristane. Photographs were taken under 10× and 60× magnifications. Normal mouse mammary fat pad (MFP) is shown as control (panels I and II). Vascularization is indicated by arrows (panel II). Expression profile of OPN was detected by immunofluorescence. Significantly higher level of OPN was observed in pristane-induced tumours whereas silencing of OPN down-regulates tumour-derived OPN expression (panel III). Expressions of MMP-9 (IV), MMP-2 (V) and MT1-MMP (VI) were determined by immunohistochemical analyses using their specific antibodies. **(B)** Expression of uPA, cellular localization of NF-κB and total phosphorylations of serine and tyrosine were analysed by immunohistochemical studies (panels I–IV). Enhanced phosphorylations of ERK and Akt were observed in pristane-induced tumours but not in OPNi-injected tumours and normal tissues (panels V and VI). Tumour sections were stained with anti-vWF antibody to visualize the angiogenesis in these tumours (panel VII). vWF positive areas are indicated by arrows. **(C)** NF-κB (upper panel) and AP-1 (lower panel)-DNA binding in tumour tissues were performed by EMSA. Six mice were used in each set of experiments.

in nude mice. We found that prolonged and continuous pristane injection in the mammary fat pad resulted in development of breast tumour growth in nude mice. We have observed the enhanced expression of OPN and other oncogenic molecules such as MMPs and uPA and enhanced angiogenesis in pristane-induced tumours. Our data showed that direct delivery of OPN-specific siRNA significantly suppressed pristane-induced tumourigenesis. Moreover, we have for the first time demonstrated the reduction of pristane-induced tumour growth and angiogenesis in OPN knock-out mice as compared to wild-type ones.

The role of host OPN in regulation of tumour growth in mice is not well defined. Previous studies have indicated that OPN deficiency in mice significantly reduced tumour metastasis in bone and lung [46]. Ohyama *et al.* has shown that deficiency of OPN in mice reduced the bone loss caused by implantation of melanoma cells into the bone marrow space [20]. In contrast, the data also showed that significant alteration of tumour metastasis in bone was not observed in OPN knockout mice [47]. Hsieh *et al.* recently noticed a marked decrease in the chemical carcinogen-induced papilloma development

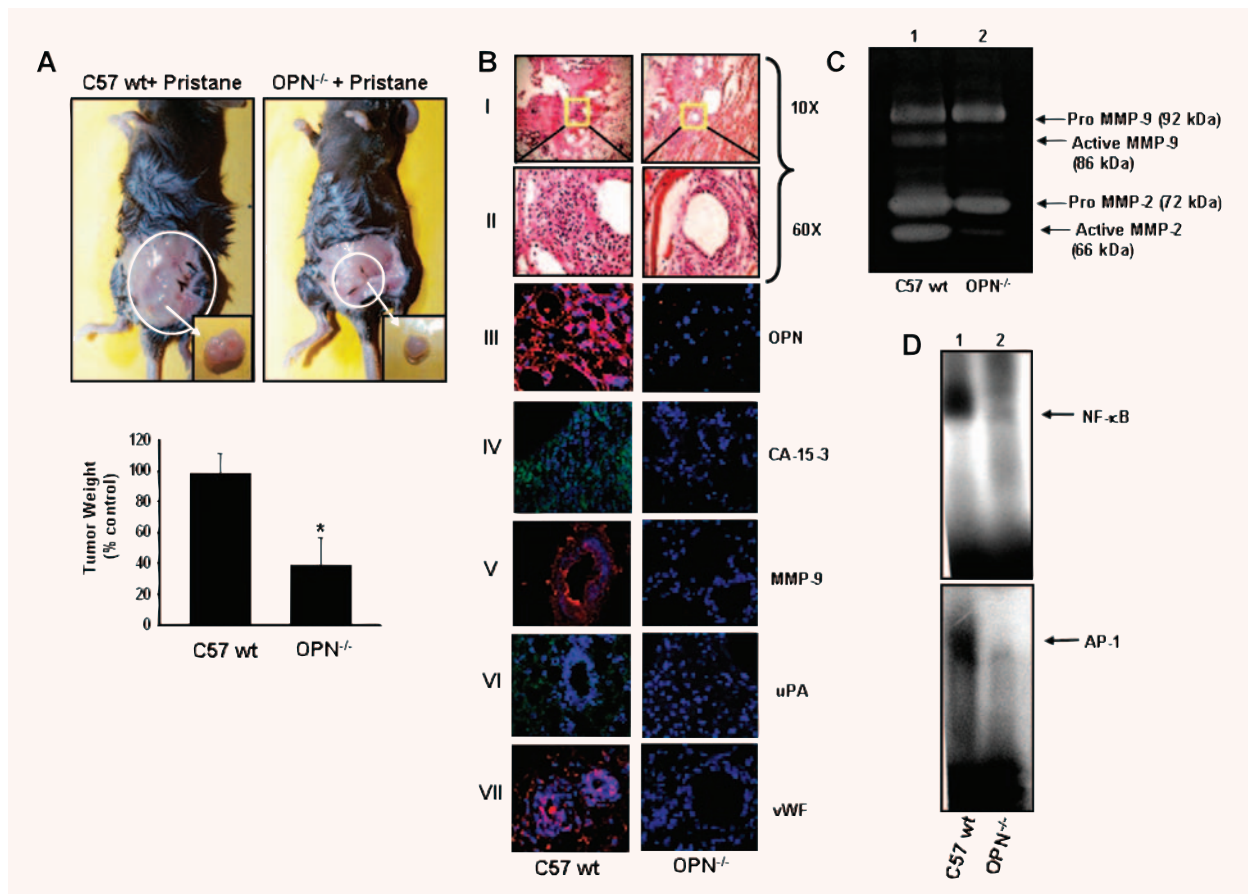


**Fig. 6** Deficiency of host OPN attenuates pristane-induced mammary carcinogenesis in OPN knockout mice. **(A)** Upper panel: Photographs showed the pristane-induced mammary tumorigenesis. Tumours are shown in inset. Lower panel, tumour weights were measured, quantified and represented in a bar graph, ( $n = 6$ ) ( $*P < 0.05$ ). **(B)** Histopathological (haematoxylin and eosin stained) micrographs of pristane-induced tumours. Photographs were taken in 10 $\times$  and 60 $\times$  magnification (panel I and II). Expression profiles of OPN (panel III), CA-15-3 (panel IV), MMP-9 (panel V), uPA (panel VI) and vWF (panel VII) were shown by immunohistochemical studies using their specific antibodies followed by staining with Cy3 or FITC conjugated IgG. Nuclei were stained with DAPI (blue). **(C)** The MMP-2 and MMP-9 expression and activation were shown by gelatin zymography. **(D)** The NF- $\kappa$ B (upper panel) and AP-1 (lower panel)-DNA bindings in tumour tissues were shown by EMSA.

in OPN<sup>-/-</sup> mice [21]. The variation of these studies might be due to the nature of tumours or origin of OPN knock out mice. In this study, we have observed that there was reduced progression of breast tumour growth and angiogenesis in OPN<sup>-/-</sup> mice.

Finally, in this study, we have demonstrated that targeting OPN might be specific and important therapeutic approach for the treatment of breast cancer. Moreover our findings suggested that pristane, a potent natural carcinogen induces breast cancer progression that could be characterized by enhanced OPN expression and silencing of this gene significantly suppresses cancer progression. Taken together, our study suggested that OPN is one of the major molecules that control the breast cancer progression. Thus, targeting OPN

might be a novel approach for the next generation of breast cancer management.

## Acknowledgements

This work was supported in part by Council of Scientific and Industrial Research, Government of India (to G.C. and S.J.). We thank Dr. B. Ramanamurthy, In-charge, Experimental Animal Facility, NCCS for breeding and maintaining the wt and knockout OPN mice. We also thank to Ms. Aswani Atre, Senior Technician, NCCS for assistance in confocal microscopy. We thank Dr. Madhumita Pradhan for helping with sample collection and confocal microscopy related works.

## References

1. **Chatterjee SK, Zetter BR.** Cancer biomarkers: knowing the present and predicting the future. *Future Oncol.* 2005; 1: 37–50.
2. **Rangaswami H, Bulbule A, Kundu GC.** Osteopontin: role in cell signaling and cancer progression. *Trends Cell Biol.* 2006; 16: 79–87.
3. **Chakraborty G, Jain S, Behera R, Ahmed M, Sharma P, Kumar V, Kundu GC.** The multifaceted roles of osteopontin in cell signaling, tumor progression and angiogenesis. *Curr Mol Med.* 2006; 6: 819–30.
4. **Higashibata Y, Sakuma T, Kawahata H, Fujihara S, Moriyama K, Okada A, Yasui T, Kohri K, Kitamura Y, Nomura S.** Identification of promoter regions involved in cell- and developmental stage-specific osteopontin expression in bone, kidney, placenta, and mammary gland: an analysis of transgenic mice. *J Bone Miner Res.* 2004; 19: 78–88.
5. **Takahashi F, Takahashi K, Shimizu K, Cui R, Tada N, Takahashi H, Soma S, Yoshioka M, Fukuchi Y.** Osteopontin is strongly expressed by alveolar macrophages in the lungs of acute respiratory distress syndrome. *Lung.* 2004; 182: 173–85.
6. **Hirama M, Takahashi F, Takahashi K, Akutagawa S, Shimizu K, Soma S, Shimanuki Y, Nishio K, Fukuchi Y.** Osteopontin overproduced by tumor cells acts as a potent angiogenic factor contributing to tumor growth. *Cancer Lett.* 2003; 198: 107–17.
7. **Jain S, Chakraborty G, Kundu GC.** The crucial role of cyclooxygenase-2 in osteopontin induced PKC $\alpha$ /c-Src/IKK $\alpha$ / $\beta$  dependent prostate tumor progression and angiogenesis. *Cancer Res.* 2006; 66: 6638–48.
8. **Cook AC, Tuck AB, McCarthy S, Turner JG, Irby RB, Bloom GC, Yeatman TJ, Chambers AF.** Osteopontin induces multiple changes in gene expression that reflect the six "hallmarks of cancer" in a model of breast cancer progression. *Mol Carcinog.* 2005; 43: 225–36.
9. **He B, Mirza M, Weber GF.** An osteopontin splice variant induces anchorage independence in human breast cancer cells. *Oncogene.* 2006; 25: 2192–202.
10. **Tuck AB, Chambers AF.** The role of osteopontin in breast cancer: clinical and experimental studies. *J Mammary Gland Biol Neoplasia.* 2001; 6: 419–29.
11. **Adwan H, Bauerle TJ, Berger MR.** Downregulation of osteopontin and bone sialoprotein II is related to reduced colony formation and metastasis formation of MDA-MB-231 human breast cancer cells. *Cancer Gene Ther.* 2004; 11: 109–20.
12. **Sliva D.** Signaling pathways responsible for cancer cell invasion as targets for cancer therapy. *Curr Cancer Drug Targets.* 2004; 4: 327–36.
13. **Cao Y, Karin M.** NF-kappaB in mammary gland development and breast cancer. *Mammary Gland Biol Neoplasia.* 2003; 8: 215–23.
14. **Filleur S, Courtin A, Ait-Si-Ali S, Guglielmi J, Merle C, Harel-Bellan A, Clézardin P, Cabon F.** siRNA-mediated inhibition of vascular endothelial growth factor severely limit tumor resistance to antiangiogenic thrombospondin-1 and slows tumor vascularization and growth. *Cancer Res.* 2003; 63: 3919–22.
15. **Takei Y, Kadomatsu K, Yuzawa Y, Matsuo S, Muramatsu T.** A small interfering RNA targeting vascular endothelial growth factor as cancer therapeutics. *Cancer Res.* 2004; 64: 3365–70.
16. **Kang CS, Zhang ZY, Jia ZF, Wang GX, Qiu MZ, Zhou HX, Yu SZ, Chang J, Jiang H, Pu PY.** Suppression of EGFR expression by antisense or small interference RNA inhibits U251 glioma cell growth *in vitro* and *in vivo*. *Cancer Gene Ther.* 2006; 13: 530–8.
17. **Pu P, Liu X, Liu A, Cui J, Zhang Y.** Inhibitory effect of antisense epidermal growth factor receptor RNA on the proliferation of rat C6 glioma cells *in vitro* and *in vivo*. *J Neurosurg.* 2000; 92: 132–9.
18. **Ait-Si-Ali S, Guasconi V, Harel-Bellan A.** RNA interference and its possible use in cancer therapy. *Bull Cancer.* 2004; 91: 15–8.
19. **Denhardt DT, Mistretta D, Chambers AF, Krishna S, Porter JF, Raghuram S, Rittling SR.** Transcriptional regulation of osteopontin and the metastatic phenotype: evidence for a Ras-activated enhancer in the human OPN promoter. *Clin Exp Metastasis.* 2003; 20: 77–84.
20. **Ohyama Y, Nemoto H, Rittling S, Tsuji K, Amagasa T, Denhardt DT, Nifuji A, Noda M.** Osteopontin-deficiency suppresses growth of B16 melanoma cells implanted in bone and osteoclastogenesis in co-cultures. *J Bone Miner Res.* 2004; 19: 1706–11.
21. **Hsieh YH, Juliana MM, Hicks PH, Feng G, Elmets C, Liaw L, Chang PL.** Papilloma development is delayed in osteopontin-null mice: implicating an antiapoptosis role for osteopontin. *Cancer Res.* 2006; 66: 7119–27.
22. **Banbura M, Ackland-Berglund C, Lee SH, Hamernik D, Jones C.** Analysis of transcriptional activation of a cyclic AMP response element by 2,6,10,14-tetramethylpentadecane (pristane) in JB6 mouse epidermal cells. *Mol Carcinog.* 1994; 11: 204–14.
23. **Anderson PN, Potter M.** Induction of plasma cell tumours in BALB-c mice with 2,6,10,14-tetramethylpentadecane (pristane). *Nature.* 1969; 222: 994–5.
24. **Armstrong MY, Ebenstein P, Konigsberg WH, Richards FF.** Endogenous RNA tumor viruses are activated during chemical induction of murine plasmacytomas. *Proc Natl Acad Sci USA.* 1978; 75: 4549–52.
25. **Janz S, Gawrisch K, Lester DS.** Translocation and activation of protein kinase C by the plasma cell tumor-promoting alkane pristane. *Cancer Res.* 1995; 55: 518–24.
26. **Horton AW, Bolewicz LC, Barstad AW, Butts CK.** Comparison of the promoting activity of pristane and n-alkanes in skin carcinogenesis with their physical effects on micellar models of biological membranes. *Biochim Biophys Acta.* 1981; 648: 107–12.
27. **Udayachander M, Meenakshi A, Krishnan RH, Padma S, Velvizhi R.** Immunoscintigraphy of MCF7 rat mammary tumour xenograft using monoclonal antibody. *Indian J Biochem Biophys.* 1994; 31: 31–5.
28. **Ohno S.** Chromosome translocations and the activation of C-myc oncogene in mouse plasmacytomas. *Gan To Kagaku Ryoho.* 1984; 11: 587–96.
29. **Akaogi J, Yamada H, Kuroda Y, Nacionales DC, Reeves WH, Satoh M.** Prostaglandin E2 receptors EP2 and EP4 are up-regulated in peritoneal macrophages and joints of pristane-treated mice and modulate TNF-alpha and IL-6 production. *J Leukoc Biol.* 2004; 76: 227–36.
30. **Philip S, Bulbule A, Kundu GC.** Osteopontin stimulates tumor growth and activation of promatrix metalloproteinase-2 through nuclear factor-kappa B-mediated induction of membrane type 1 matrix metalloproteinase in murine melanoma cells. *J Biol Chem.* 2001; 276: 44926–35.

31. **Hazama A, Fan HT, Abdullaev I, Maeno E, Tanaka S, Ando-Akatsuka Y, Okada Y.** Swelling-activated, cystic fibrosis transmembrane conductance regulator-augmented ATP release and Cl<sup>-</sup> conductances in murine C127 cells. *J Physiol.* 2000; 523: 1–11.
32. **Sclimenti CR, Baba EJ, Calos MP.** An extrachromosomal tetracycline-regulatable system for mammalian cells. *Nucleic Acids Res.* 2000; 28: e80.
33. **Teramoto H, Castellone MD, Malek RL.** Autocrine activation of an osteopontin-CD44-Rac pathway enhances invasion and transformation by H-RasV1 2. *Oncogene.* 2005; 24: 489–501.
34. **Chakraborty G, Rangaswami H, Jain S, Kundu GC.** Hypoxia regulates cross-talk between syk and Ick leading to breast cancer progression and angiogenesis. *J Biol Chem.* 2006; 281: 11322–31.
35. **Philip S, Kundu GC.** Osteopontin induces nuclear factor kappa B-mediated promatrix metalloproteinase-2 activation through I kappa B alpha /IKK signaling pathways, and curcumin (diferuloylmethane) down-regulates these pathways. *J Biol Chem.* 2003; 278: 14487–97.
36. **Gillespie DL, Whang K, Ragel BT, Flynn JR, Kwily DA, Jensen RL.** Silencing of hypoxia inducible factor-1 $\alpha$  by RNA interference attenuates hman glioma cell growth *in vivo.* *Clin Cancer Res.* 2007; 13: 2441–8.
37. **Garcia FU, Urbanska K, Koltowski L, Reiss K, Sell C.** Insulin-like growth factor-i produced by seminal vesicles: relationship to intraepithelial basal cell hyperplasia in the prostate. *Clin Cancer Res.* 2007 13: 3140–6.
38. **Sotiriou C, Wirapati P, Loi S, Harris A, Fox S, Smeds J, Nordgren H, Farmer P, Praz V, Haibe-Kains B, Desmedt C, Larsimont D, Cardoso F, Peterse H, Nuyten D, Buyse M, Van de Vijver MJ, Bergh J, Piccart M, Delorenzi M.** Gene expression profiling in breast cancer: understanding the molecular basis of histologic grade to improve prognosis. *J Natl Cancer Inst.* 2006; 98: 262–72.
39. **Pass HI, Lott D, Lonardo F, Harbut M, Liu Z, Tang N, Carbone M, Webb C, Wali A.** Asbestos exposure, pleural mesothelioma, and serum osteopontin levels. *N Engl J Med.* 2005; 353: 1564–73.
40. **Dolle L, Depypere HT, Bracke ME.** Anti-invasive/anti-metastasis strategies: new roads, new tools and new hopes. *Curr Cancer Drug Targets.* 2006; 6: 729–51.
41. **Moore S, Cobleigh MA.** Targeting metastatic and advanced breast cancer. *Semin Oncol Nurs.* 2007; 23: 37–45.
42. **Folkman J.** Angiogenesis: an organizing principle for drug discovery? *Nat Rev Drug Discov.* 2007; 6: 273–86.
43. **Jain S, Chakraborty G, Bulbule A, Kaur R, Kundu GC.** Osteopontin: an emerging therapeutic target for anticancer therapy. *Expert Opin Ther Targets.* 2007; 11: 81–90.
44. **Chakraborty G, Jain S, Kundu GC.** Osteopontin promotes VEGF dependent breast tumor growth and angiogenesis via autocrine and paracrine mechanisms. *Cancer Res.* 2008; 68: 152–61.
45. **Cogliano VJ, Grosse Y, Baan RA Straif K, Secretan MB, El Ghissassi F; Working Group for Volume 88.** Meeting report: summary of IARC monographs on formaldehyde, 2-butoxyethanol, and 1-tert-butoxy-2-propanol. *Environ Health Perspect.* 2005; 113: 1205–8.
46. **Nemoto H, Rittling SR, Yoshitake H, Furuya K, Amagasa T, Tsuji K, Nifuji A, Denhardt DT, Noda M.** Osteopontin deficiency reduces experimental tumor cell metastasis to bone and soft tissues. *J Bone Miner Res.* 2001; 16: 652–9.
47. **Natasha T, Kuhn M, Kelly O, Rittling SR.** Override of the osteoclast defect in osteopontin-deficient mice by metastatic tumor growth in the bone. *Am J Pathol.* 2006; 168: 551–61.